International Journal of Development and Sustainability
ISSN: 2168-8662 – www.isdsnet.com/ijds
Volume 3 Number 4 (2014): Pages 662-678
ISDS Article ID: IJDS13052405

Development of a regional landslide prediction model for Kerio Valley in Kenya

Joel Kibiiy [1*], Kipyegon Koskei [2], Cornelius Sitters [2], Julius Ndambuki [4]

[1] *Visiting Research Fellow, Department of Civil Engineering, Tshwane University of Technology, South Africa: Private Bag, X680, Pretoria 0001 South Africa*
[2] *Department of Civil and Structural Engineering, Moi University, P.O. Box 3900 - 30100 Eldoret, Kenya*
[3] *Department of Civil Engineering, Tshwane University of Technology, Private Bag, X680, Pretoria 0001 South Africa*

Abstract

Occurrences of rainfall induced landslides coincide in time with the period of high persistence of heavy wet spells and in spatial locations where vegetative cover has been denuded. A landslide prediction model was formulated and calibrated by simulation of previous landslide occurrences and then applied in scenario analyses to establish the effects of rainfall persistence and land use changes on slope stability in the western escarpment of the Kerio Valley in Kenya. Long term daily rainfall input was obtained using a rainfall generator. HYDRUS 1D model was applied in soil moisture analysis. An EXCEL spreadsheet infinite slope model was developed for model calibration. ILWIS GIS model was used to map spatial distribution of slope stability. The model successfully modelled the occurrence of previous landslide events. Results indicate that rainfall totals and wet spell persistence contribute to increase in unstable areas. Assessment of slope stability under different land uses showed that if the entire study area were completely forested, then the unstable and critical areas would be 0.05% and 1.81% respectively, but would be 0.69% and 5.35% respectively if it were completely under agriculture.

Keywords: Landslide Prediction Model; HYDRUS 1D; ILWIS GIS

Cite this article as: Kibiiy, J., Koskei, K., Sitters, C. and Ndambuki, J. (2014), "Development of a regional landslide prediction model for Kerio Valley in Kenya", *International Journal of Development and Sustainability*, Vol. 3 No. 4, pp. 662-678.

[*] Corresponding author. *E-mail address:* Kibiiy@yahoo.com

1. Introduction

Landslides represented about 5% of all natural disasters worldwide between 1990 and 2005 (Kanungo et al., 2006). In Kenya, landslides frequently occur when the country experiences heavy rainfall and often lead to loss of life and destruction of property (Standardmedia, 2012; Standardmedia, 2011; BBC news, 2010; Standardmedia, 2010). Numerous factors contribute to slope failures in mountainous areas. However, intense rainfall (Lakhan, 2009) is a trigger in both shallow and deep-seated landslides since rain water percolating the slopes increases the soil water content and reduces in situ matric suction, resulting in a decrease in the effective stress in the slope soils. This may induce slope failures when the critical pore water pressure threshold is exceeded (Corominas and Moya, 1999).

Land use change has been recognized as the most important factor influencing the occurrence and re-activation of landslides triggered by rainfall. The relation between landslide and vegetation cover is extremely important and should not be underestimated. Vegetation influences slope stability parameters such as cohesion, angle of internal friction, weight of the slope-forming material and pore-water pressure (Karsli et al., 2008). Shallow slope failures occurred in Northern Ontario after forest clearing and the major causes of these slope failures was attributed to a decrease in evapotranspiration and decaying of the root system (Eigenbrod and Kaluza, 1997). It is thus important to investigate the hydrological, land use and soil factors that have a bearing on slope instabilities by using modelling approaches so as to provide an insight into the causes and spatial distribution of landslides.

In addition to cost, available landslide models often have requirements that make it difficult to run in situations of limited data. This paper presents the theoretical background, the methods used in development, modelling and simulation, followed by interpretation and discussion of results. Finally, conclusions and recommendations for further research are given.

2. Modeling and scenario analyses

2.1. Study area

The study area is part of the highland escarpment of the Great Rift Valley located in Elgeyo-Marakwet County in Kenya (Figure 1). It lies within the coordinates of 35^0 29'E 0^0 51'N and 35^0 43'E 1^0 19'N. The altitude of the area ranges from about 1000 meters above sea level (a.s.l) in the valley floor to about 3000 meters a.s.l in the highlands. The average temperature at the valley is around 26 centigrade and 6 to 18 centigrade at the highlands. Annual rainfall ranges from 1000 mm at the basin of the valley to 1600 mm in the highlands. Annual evaporation rate is about 2000 mm in the valley and 1300 mm in the highlands (Muchemi et al., 2002). During heavy rains, the escarpment suffers from landslides and soil erosion while the valley floor suffers from floods and deep gullies. These threaten the suitability and sustainability of the environment for human habitation. Mokwo village is in the highlands. It is endowed with fertile dark-brown loamy soils which are well drained.

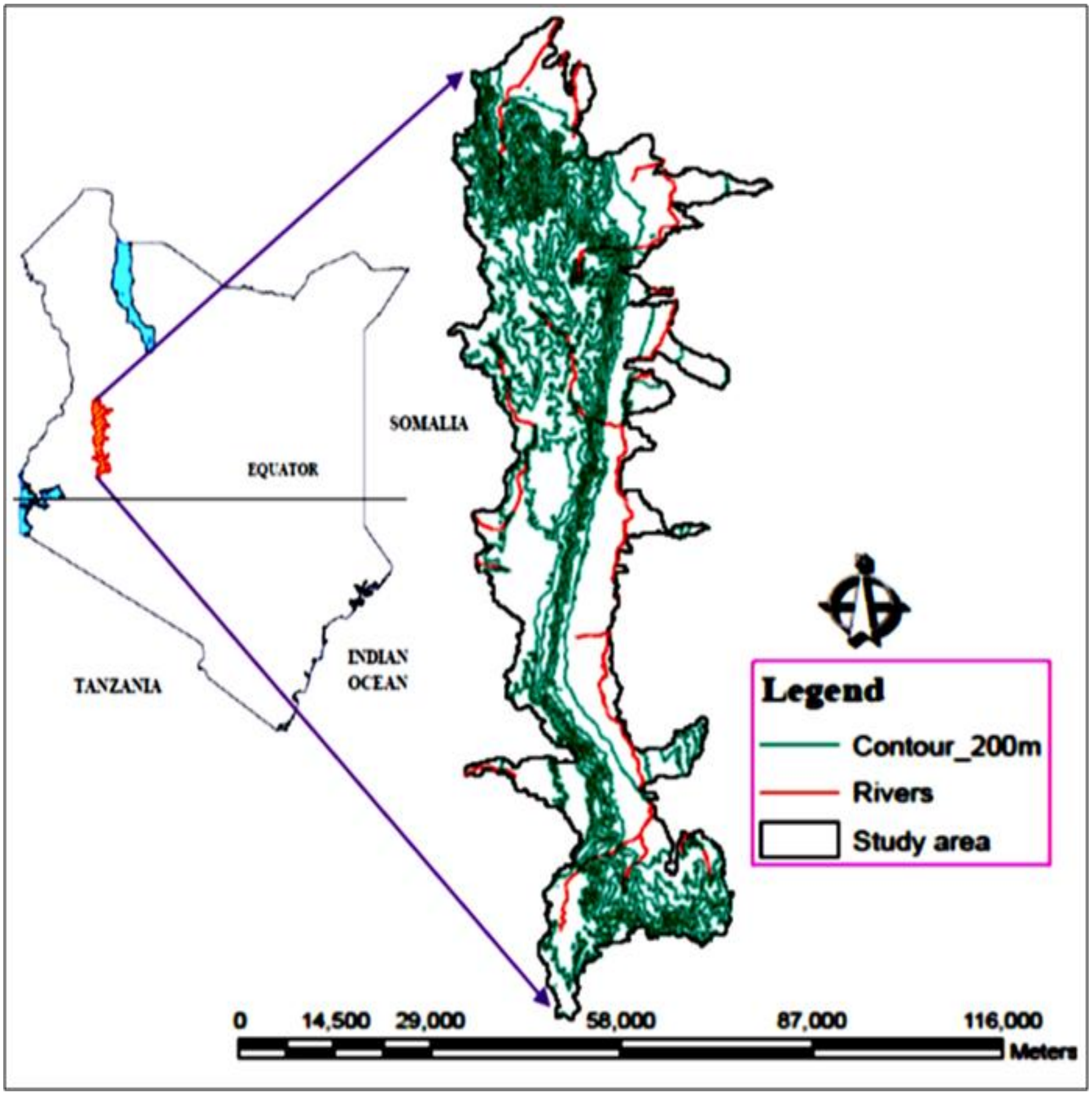

Figure1. Location of study area in Kenya

2.2. Soil moisture modeling using HYDRUS 1D

The rainfall necessary to drive the system was generated using stochastic rainfall generating model (Koskei, 2013). The state of soil moisture after a wet spell was obtained using a one-dimensional mixed form of Richard's equation describing the uniform movement of water in a partially saturated rigid porous medium with assumptions that the air phase plays an insignificant role in the liquid flow process and that water flow due to thermal gradients is neglected (Šimůnek et al., 2009).

$$\frac{\partial \theta}{\partial t} = \frac{\partial}{\partial z}\left[K\left(\frac{\partial h}{\partial z} + \cos\alpha\right)\right] - S \qquad (1)$$

where h is the pressure head [L], θ is the volumetric water content [L^3L^{-3}], t is time [T], z is the spatial coordinate [L] (positive upward), S is the sink term [$L^3L^{-3}T^{-1}$], defined as the volume of water removed from a unit volume of soil per unit time due to plant water uptake (Feddes et al., 1978), α is the angle between the flow direction and the vertical axis (i.e., $\alpha = 0^0$ for vertical flow, $\alpha = 90^0$ for horizontal flow, $0 < \alpha < 90^0$ for inclined flow) and K is the unsaturated hydraulic conductivity [LT^{-1}].

Richards' equation does not have a general analytical solution, and must therefore be solved numerically. The HYDRUS 1D software was used for this purpose. It is a finite difference programme where the soil profile is first discretized into $N - 1$ adjoining elements (Figure 2) perpendicular to the soil surface with the ends of the elements located at the nodal points; N is the number of nodes.

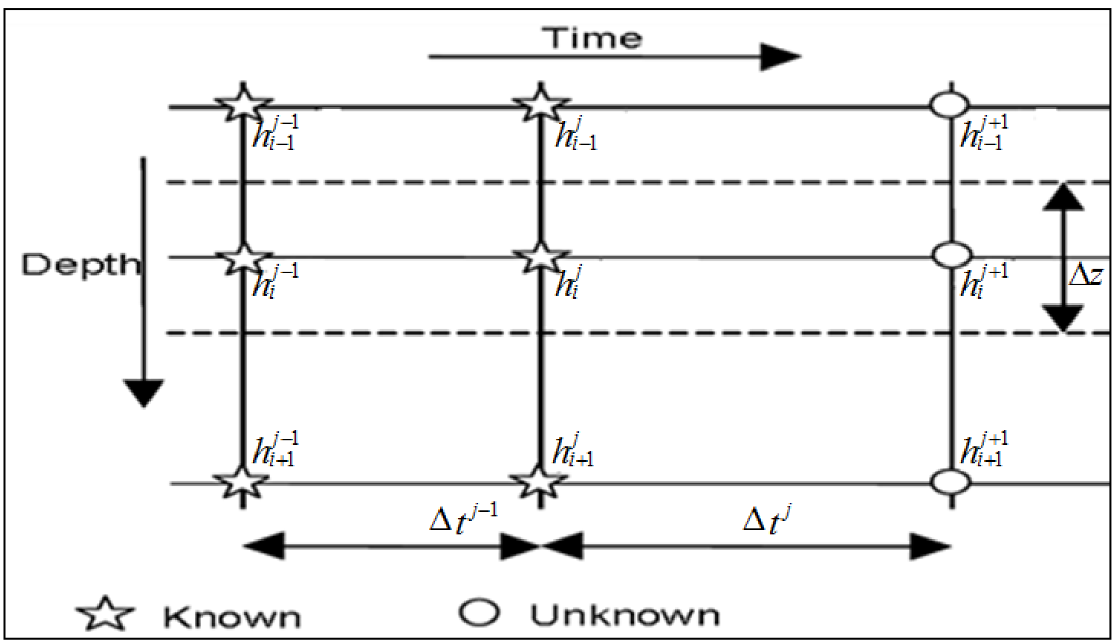

Figure 2. Spatial and temporal discretization scheme used in solving Richard's equation (Source: Gurrapu, 2005)

A mass-lumped linear finite elements scheme was used for discretization of the mixed form of the Richards' equation resulting in an equivalent and somewhat standard finite difference scheme (e.g., Vogel et al., 1996);

$$\frac{\theta_i^{j+1,k+1}-\theta_i^j}{\Delta t}=\frac{1}{\Delta z}\left(K_{i+1/2}^{j+1,k}\frac{h_{i+1}^{j+1,k+1}-h_i^{j+1,k+1}}{\Delta z_i}-K_{i-1/2}^{j+1,k}\frac{h_i^{j+1,k+1}-h_{i-1}^{j+1,k+1}}{\Delta z_{i-1}}\right)+\frac{K_{i+1/2}^{j+1,k}-K_{i-1/2}^{j+1,k}}{\Delta z}\cos\alpha-S_i^j \quad (2)$$

in which subscripts $i-1$, i, and $i+1$ indicate the position in the finite difference mesh; superscripts k and $k+1$ denote the previous and current iteration levels, respectively; and superscripts j and $j+1$ represent the previous and current time levels, respectively. Equation (2) is based on a fully implicit discretization of the time derivative, and is solved using a Picard iterative solution scheme.

The flux components were calculated only at each node N, with the upper boundary condition chosen as atmospheric with surface runoff while lower boundary condition was chosen as constant flux, $q=0$, assuming rock level. The initial condition was specified in terms of the volumetric water content and an assumed value of 0.2 was set.

$$q_i^{j+1}=\frac{-K_{i+1/2}^{j+1}\left(\frac{h_{i+1}^{j+1}-h_i^{j+1}}{\Delta z_i}+1\right)\Delta z_{i-1}-K_{i-1/2}^{j+1}\left(\frac{h_i^{j+1}-h_{i-1}^{j+1}}{\Delta z_{i-1}}+1\right)\Delta z_i}{\Delta z_{i-1}+\Delta z_i} \quad (3)$$

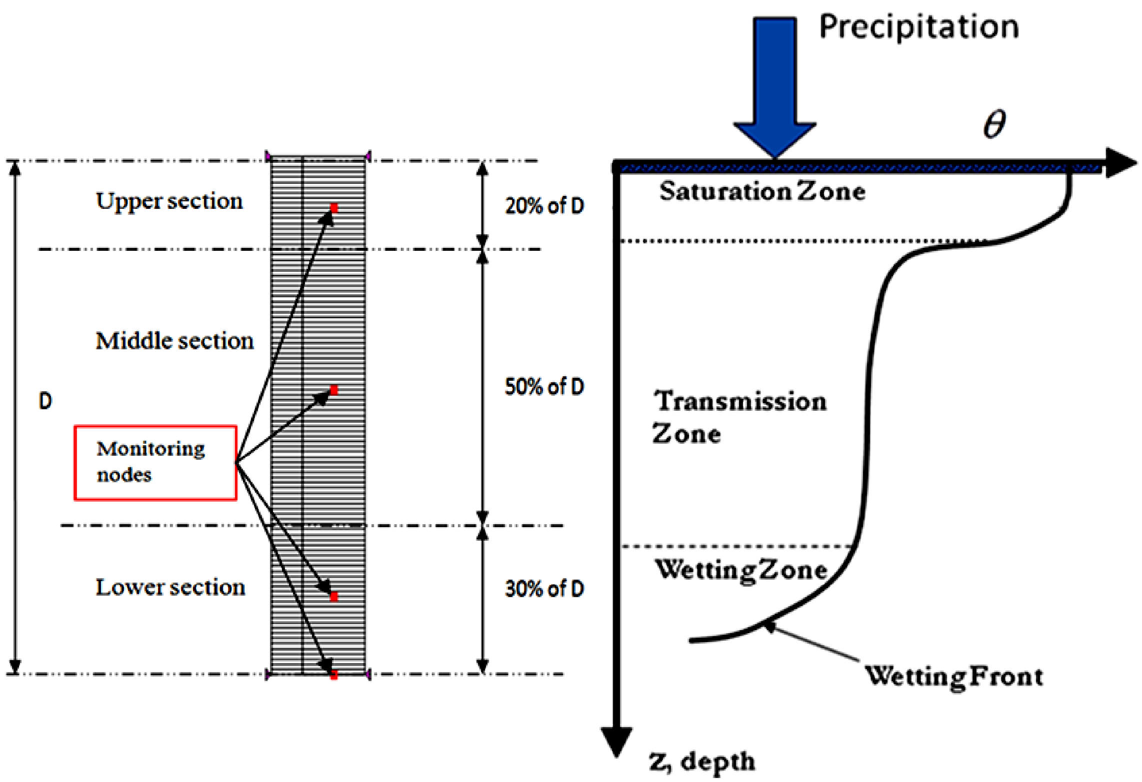

Figure 3. Descretization of soil layer in HYDRUS 1D model and the infiltration zones

The soil layer was discretized into one hundred and one equidistant nodes. The soil moisture simulation was monitored in nodes 11, 46, 86 and 101. The modelled water content in nodes 11, 46 and 86 represented average water content in the three soil zones (Figure 3). The upper section which is highly affected by weather conditions was represented by 20% of soil layer thickness while the lower section that represents water accumulation was represented by 30% of soil thickness. The middle section (transmission zone) took 50% the thickness of soil layer.

The HYDRUS 1D model requires temporal data that include time, precipitation rate, potential evapotranspiration rate, and absolute value of the minimum allowed pressure head at the soil surface which should be selected such that the corresponding water content is at least 0.005 higher than the residual water content (Van Genuchten,1980).

2.3. Slope stability model

In the infinite slope model, failure occurs when soil shear stress exceeds soil shear strength. Factor of safety F_s at any point in a soil layer is obtained as the ratio between the soil shear strength τ_r and shear stress τ (Christanto, 2008).

$$F_s = \frac{\tau_r}{\tau} = \frac{c_t + \sigma_z^{'} \tan\phi}{\sigma_z \tan\beta} \qquad (1)$$

where; $\sigma_z^{'}$ =effective normal stress, σ_z = total normal stress, c_t = total cohesion strength, ϕ = angle of internal friction, β = slope obliquity.

For partially saturated soils, there exists suction stress that increases the soil effective shear resistance on a slope. Therefore, infinite slope stability equation has to be modified to take into consideration suction stress. A generalized effective stress equation in soil that unifies both saturated and unsaturated conditions was proposed by Lu and Likos (2004, 2006) as

$$\sigma_z^{'} = (\sigma_z - u_a) - \sigma^s \qquad (1)$$

where u_a is the pore air pressure, σ_z = effective normal stress, σ_z = total normal stress, σ^s = matric suction stress at failure plane.

Equation (5) is used to replace the effective normal stress in equation (4) (Duncan and Wright, 2005), resulting in an equation describing stability of a slope under any soil saturation condition i.e.,

$$F_s = \frac{c_t + \left\{(\sigma_z - u_a)\cos^2\beta - \sigma^s\right\}\tan\phi}{\sigma_z \cos\beta \sin\beta} = \frac{c_t + \left\{(\gamma Z - \gamma_w Z_w)\cos^2\beta - \sigma^s\right\}\tan\phi}{\gamma Z \cos\beta \sin\beta} \qquad (1)$$

where Z, Z_w = depths of partially/ saturated soil and water table above failure plane, γ, γ_w = unit weight of soils and water respectively, u_a is assumed equal to zero.

The flow chart for the infinite slope model is given in Appendix A. The formulation was implemented both in ILWIS GIS model (mapping function) and in Ms-EXCEL comprising the LPM for calibration and identification of critical mapping days.

2.4. Spatial modelling using ILWIS GIS

ILWIS GIS model was applied for spatial mapping of unstable areas (Pack *et al.*, 2001). ILWIS GIS provides a platform for formulating mapping equations such as infinite slope model. It requires raster maps of soil and topographical properties and also inputs of soil moisture from a hydrological model. The mapping function in ILWIS GIS model was formulated taking into consideration spatial variation in components of hydrology and topography that affect stability of slopes. These components include water flow flux, soil moisture, slope, land use and soil type. The formulated methodology was calibrated using previous landslide occurences. Calculation of slope stability in ILWIS GIS is done on a pixel basis and the effect of the neighbouring pixels is not considered resulting in a hazard map of safety factors (Van Westen and Terlien, 1996). The flow chart for Landslide Prediction Model (LPM) is shown in Appendix B.

2.5. Model calibration

The formulated model was calibrated on the landslides that occurred previously at the escarpment near Mokwo village. The area has loam soil with an average thickness of about 1.5m. The major land use activity in the area is intensive agriculture (Muchemi, 2002; Kenya soil survey, 1997). The escarpment in the area slopes at an angle of around 40 degrees. The rainfall data for HYDROID 8935184 rainfall station was used for simulation as it was the nearest meteorological station to the landslide occurrence site.

Sensitivity analysis was conducted using HYDRUS 1D model and Ms-EXCEL infinite slope model to establish influence of soil and topographic parameters on slope stability. Since all the parameters had an effect on state of slope stability, it was decided to calibrate the model by multiplying formulated factor of safety function with a constant so as to force the model to indicate failure on 29th April. A numerical constant 0.55 gave the anticipated results.

3. Results and discussion

3.1. Model calibration

The variation with time of volumetric water content and suction stress in the soil layer are depicted in Figure 4 and Figure 5 respectively. In factor of safety analysis and spatial mapping, only suction stress results for top of bedrock was used since failure plane in this study was assumed to coincide with this point.

Variation of factor of safety (F_S) with time was undertaken using formulated Ms-EXCEL infinite slope model. The F_S model value for 29th April was found to be overstated since it is above the critical value of 1. Overestimation of F_S may have been caused by overestimated angle of friction, underestimated slope angle, underestimated depth, or overestimated cohesion.

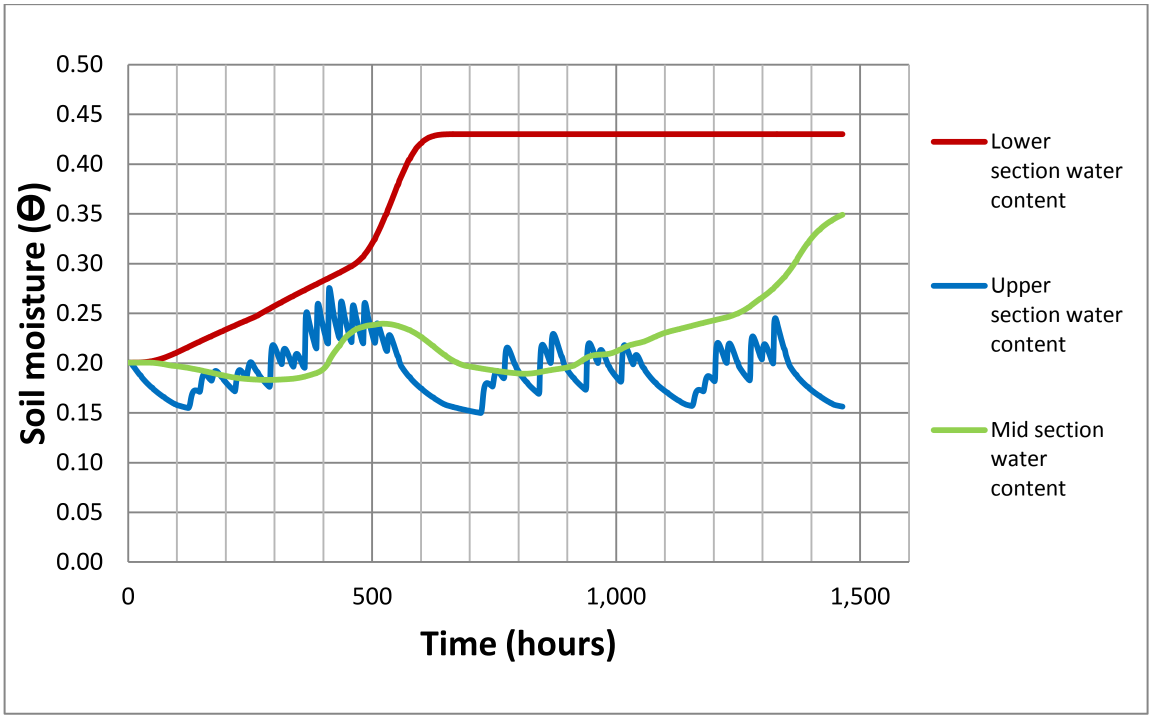

Figure 4. Redistribution of Soil water for loam soil of thickness of 1.5 m at Mokwo village

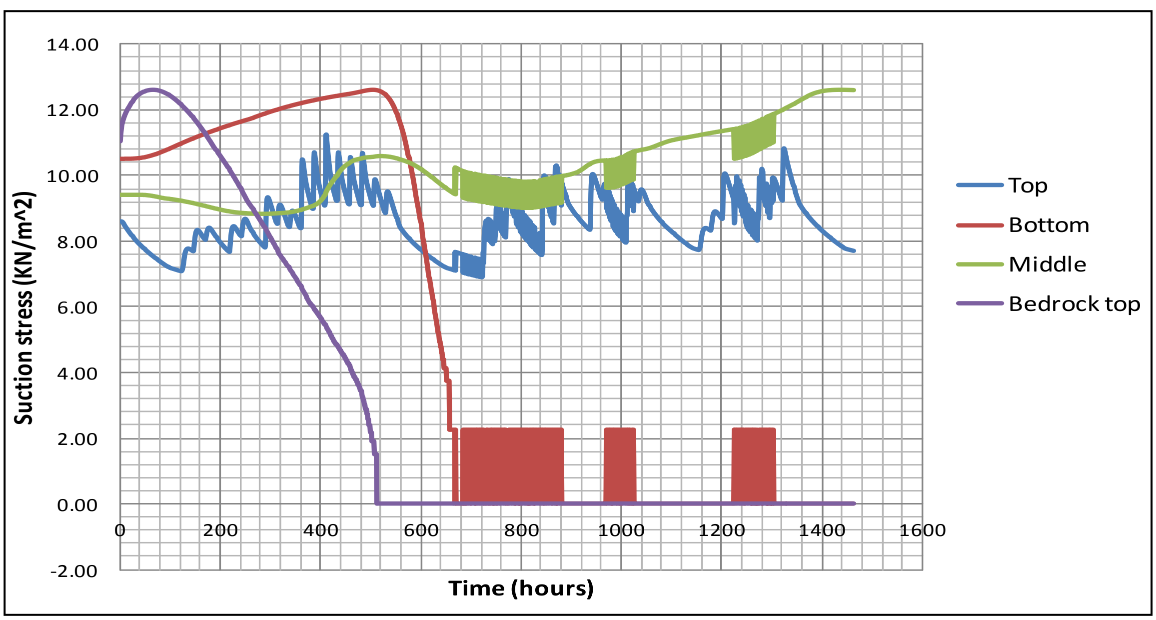

Figure 5. Variation of suction stress for loam soil of depth 1.5m at Mokwo village

Table 1 shows the results of the sensitivity analysis while Figure 6 shows the calibrated results.

Table 1. Sensitivity of model to parameter change

Parameter name	Parameter Value adopted	Increasing parameter value by 25%	Fs	Decreasing parameter value by 25%	Fs
Angle of friction	28	35	1.9	21	1.6
Soil cohesion	16	20	2.0	12	1.4
Soil depth	1.5	1.88	1.4	1.13	2.2
Slope angle	40	50	1.55	30	2.0

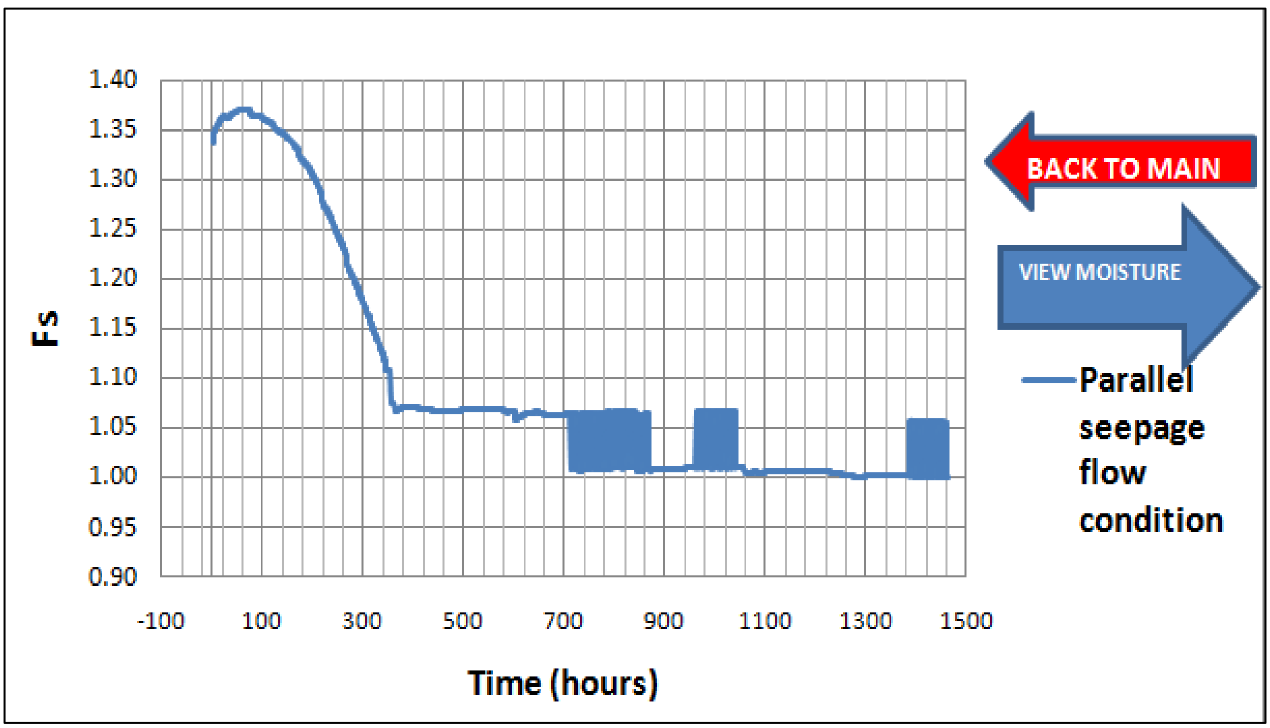

Figure 6. Variation of F_s for loam soil of depth 1.5 m on a 40^0 slope

A mapping function formulated from infinite slope equation was used in generation of the hazard maps. Figure 7 shows hazard map for the Mokwo area at the time of a landslide on 29th April 2007 (around time 700 hours).

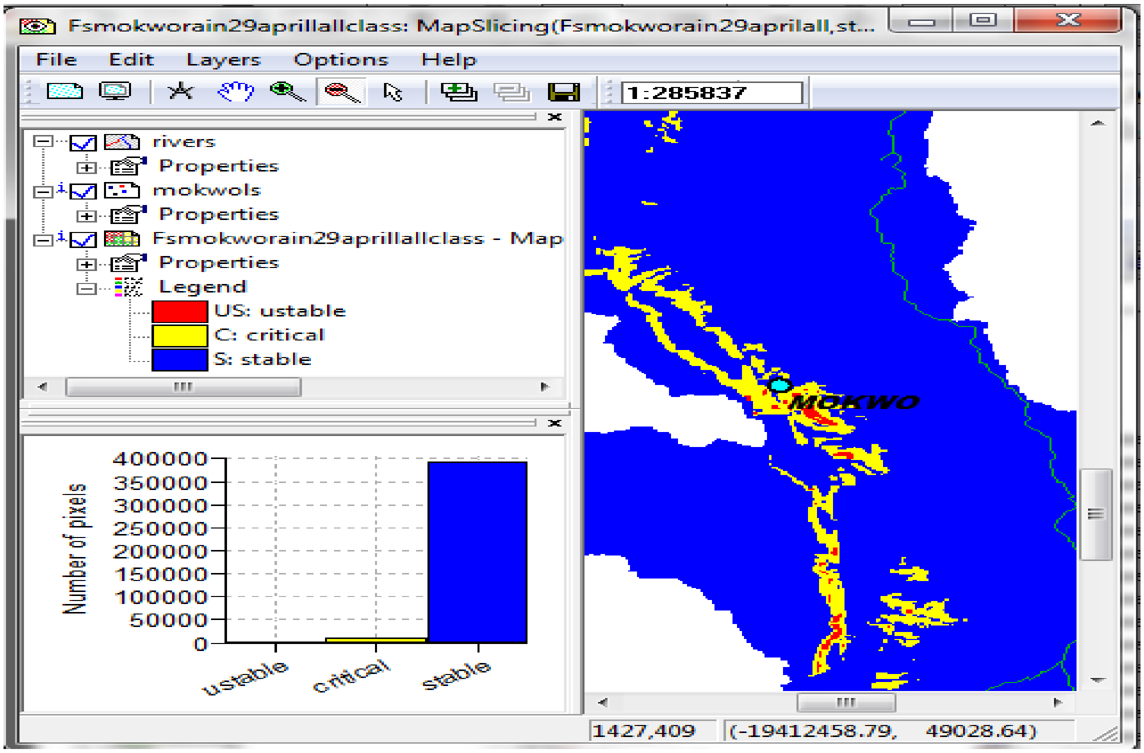

Figure 7. Hazard map for Mokwoarea at time of landslide on 29th April 2007 (time 700 hours)

3.2. Scenario analysis for slope stability assessment

Two aspects were analysed for landslides triggering conditions. These were the rainfall persistence and land use changes.

3.2.1. Evaluating effects of rainfall persistence on slope stability

The rainfall that caused landslides in the 2007, 2010, 2011 and 2012 had a cumulative total of between 420 and 460 mm for the months of April and May. Therefore generated rainfalls having totals greater than 420mm for the months of April and May were used for analysis.

HYDRUS 1D model was run on the generated rainfall to create temporal soil parameters that were then applied in ILWIS GIS software for generation of spatial slope instability (hazard) map. The effect of rainfall persistence on slope stability was demonstrated by generating hazard maps for different days in the analysis period using ILWIS GIS and the generated percentages of stable, critical and unstable areas are as shown in the Table 2.

Table 2. Statistical analysis for stability classifications in ILWIS GIS

	STABILITY RESULTS				
		Percentage area (%)		**Area (m^2)**	
date	**stability class**	**evenly**	**skewed**	**evenly**	**skewed**
13th April	unstable	0.24	0.24	8028326.2	8002649.2
	critical	3.7	4	12372660.2	133871055.2
	stable	96.06	95.76	3213033709.9	3202916991.9
21st April	unstable	0.86	0.84	28749624.4	28141936.5
	critical	4.74	4.73	158546603.6	158212803.3
	stable	94.4	94.43	3157494468.4	31584435956.5
6th May	unstable	1.5	1.48	50309702.9	49642102.2
	critical	5.18	5.08	173113992.9	170049876.9
	stable	93.32	93.43	3121367000.6	3125098717.2
23rd May	unstable	0.33	0.57	11546068.2	19685661.2
	critical	3.38	3.36	117300863.9	116530555.4
	stable	96.28	96.07	3338345782.0	3330976497.5

3.2.2. Evaluating Effects of Land Use Change on Slope Stability

The analysis to test the effect of landuse change considered the stabilizing effect of roots for two assumed scenarios:

- Adoption of (pine) forest as a sole land use in the entire study area.
- Adoption of agriculture (maize farming) as a sole land use in the entire study area.

In the first scenario, it was assumed that the study area was covered entirely with pine forest. The adopted values for root tensile strength and root area ratio (RAR) are 30 MPa and 0.0075 respectively (Norris et al., 2008; De Baets et al, 2008). In the second scenario, it was assumed that the entire study area consisted of a maize plantation. April is the maize planting period in the study area. A root tensile strength and RAR of 5 MPa and 0.001 were adopted respectively. The resulting hazard maps are shown in Figure 8.

The percentage of unstable and critical areas for pine forest was found to be 0.05% and 1.81% respectively while for maize it was 0.69% and 5.35% respectively.

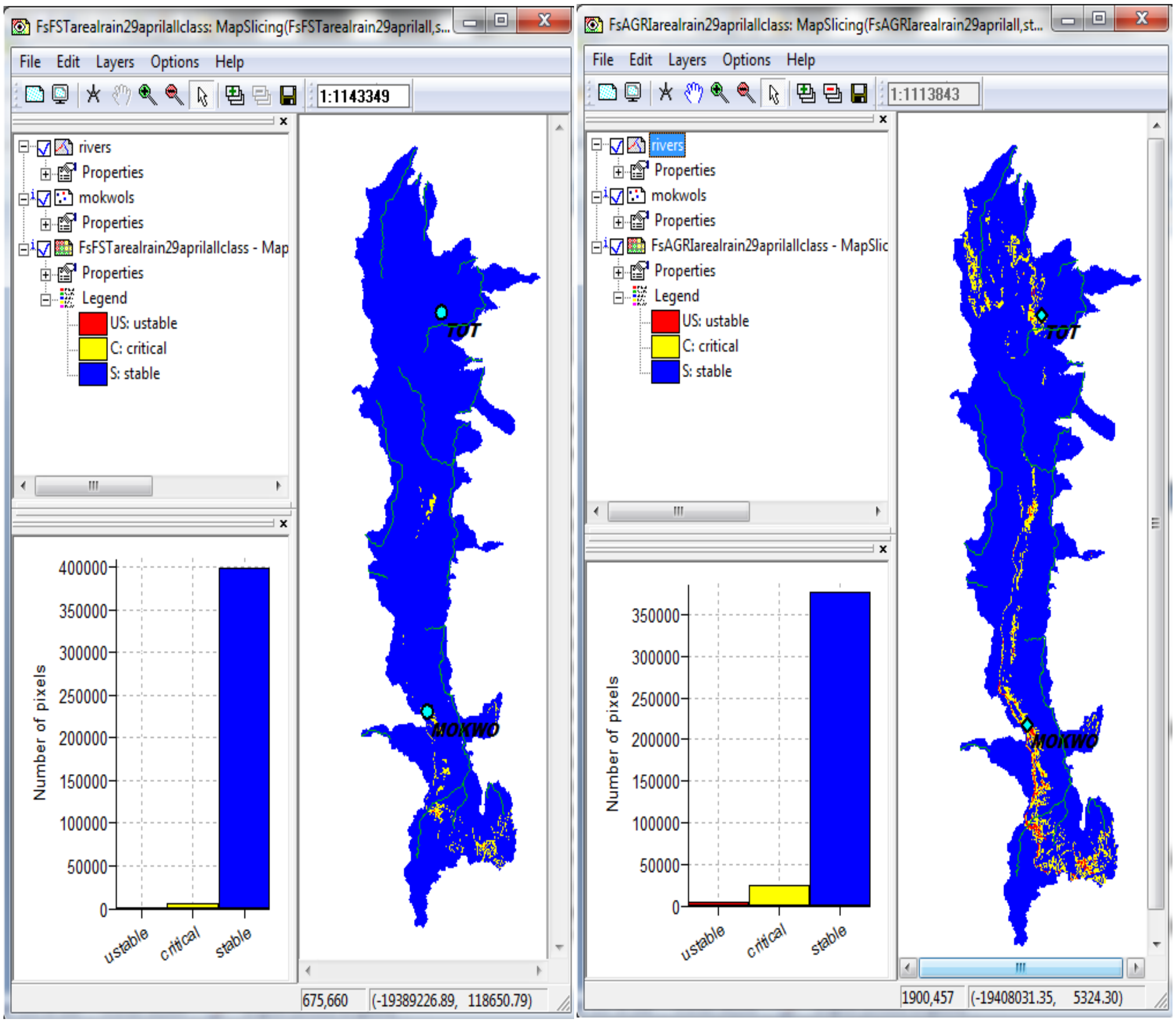

(a) (b)

Figure 8. Scenario hazard map of study area on 29th April 2007: (a). Forest cover; (b). Agriculture

3.3. Discussion

Soil moisture content in the soil layer varies with depth (Figure 4). The uppermost soil layer gets moisture directly from rainfall and loses it faster than the lower layers due to its direct exposure to solar radiation and wind. After the onset of the rainy season, water content of the lower layers would build up gradually to saturation because the bedrock would not allow further percolation of soil water. Similarly, the suction stress varies with the water content (Figure 5). Suction stress of the upper soil layers is high and fluctuates continuously with the water content. In the bottom section, soil suction has much lower values and tends to zero in many places due to high water content.

The values of F_S based on site soil parameters was found to be slightly higher for failure at the desired times. Since a sensitivity analysis did not reveal a dominant parameter, the model was forced by multiplying with a constant. The resulting model was able to produce satisfactory hazard map that included the landslide event at time of 29th April 2007 (around time 700 hours) in the unstable areas (Figure 6 and Figure 7).

It was established that rainfall intensity in the study area follows a gamma distribution in which 60% of the rainfall tends to fall within the first 20 minutes (Koskei, 2013). The main soil type in the study area is clay loam with characteristically low infiltration rates that can easily be exceeded by the rainfall intensity resulting in the generation of high surface runoff. This explains why individual storms with high total amount of rainfall do not necessarily produce high percentages of unstable areas.

Landuse type also has a great influence on the slope stability. The adoption of pine forest in the study area would result in much smaller area being unstable or in critical state as compared to that for maize plantation in April.

4. Conclusions and recommendations

4.1. Conclusions

Landslide hazards can be systematically assessed using different methods depending on the available data and resources. For this study, a model was developed to suit available resources.

The results obtained from this study were fairly conclusive that high persistence of heavy rainfall was a major contributor to landslides in the study area. Persistent high rainfall would result in more slope failures. Scenario analysis involving pine forest and maize plantations for land use respectively confirmed the importance of vegetation roots in reinforcing of soils on slopes. The formulated landslide prediction methodology could provide a basis for modelling the occurrence of rainfall induced landslides since most of the standard models are commercial. Information provided by hazard maps could form a basis of decision making by relevant authorities for reducing, preventing, mitigating and avoiding losses caused by landslides.

4.2. Recommendations

Most of the analyses were based on values obtained from the literature and may not accurately correspond to field values for the study area. These include: soil types and their properties, RAR values and root distribution with depth. This may have led to under- or over-estimation of F_S in slope stability analysis.

It is recommended that all future landslides in Kenya should be geo-referenced and documented by relevant institutions to facilitate quality assessment and validation in future studies. Research is also recommended to accurately establish soil types and their properties and values of other landslide related parameters.

Acknowledgement

The research was supported with funds from the VLIR Programme at Moi University.

References

BBC news (2010), "Kenya villagers die in Rift Valley landslide", Page last updated at 18:50 GMT, Friday, 30 April 2010, Available: http://news.bbc.co.uk/2/hi/8655298.stm; Accessed on 17th December, 2013.

Chow, V.T., Maidment, D.R. and Mays, L.W. (1988), *Applied Hydrology*, McGraw-Hill, New York.

Christanto, N. (2008), "Hydrological-slope stability modeling for landslide hazard assessment by means of GIS and remote sensing data", Msc thesis, Faculty of Geography, Gadjah Mada University, Yogyakarta.

Corominas, J. and Moya, J. (1999), "Reconstructing recent landslide activity in relation to rainfall in the Lobregat River basin, Eastern Pyrenees, Spain", *Journal of Geomorphology*, Vol. 30 No.1-2, pp.79-93.

De Baets, S., Poesen J., Knapen A., Barberá G.G. and Navarro J.A. (2008), "Root characteristics of representative Mediterranean plant species and their erosion-reducing potential during concentrated runoff", *Journal of Plant Soil*, Vol. 294, pp.169-183.

Duncan, J.M. and Wright S.G. (2005), *Soil strength and slope stability*, John Wiley, Hoboken, NJ.

Feddes, R.A., Kowalik, P.J. and Zaradny, H. (1978), *Simulation of field water use and crop yield*, John Wiley & Sons, New York, NY.

Gurrapu, S. (2005), "Estimation of soil moisture in unsaturated zone and irrigation scheduling", A master thesis at department of applied mechanics & hydraulics, National Institute of Technology Karnataka, *(A Deemed University)*INDIA, available at: http://www.scribd.com/doc/16834520/14/Figure-3-4-Spatial-and-temporal-discretization-used-to-solve-Richard%E2%80%99s-equation*;* accessed on 24 May 2013.

Kanungo, D.P., Arora, M.K., Sarkar, S. and Gupta, R.P. (2006), "A comparative study of conventional, ANN black box, fuzzy and combined neural and fuzzy weighting procedures for landslide susceptibility zonation in Darjeeling Himalayas", *Engineering Geology*, Vol.85 pp. 347–366.

Kenya soil map. Kenya soil survey (1997), "Kenya soil".

Koskei, K. (2013), "Susceptibility modeling of rainfall induced landslides", Msc. Thesis. Moi University, Eldoret, Kenya.

Lakhan R.R. (2009), "Landslide susceptibility mapping through enhanced dynamic slope stability analysis using earth observing satellite measurements", Ph.D. dissertation, University of New Hampshire, 201 pages; 3383325: ISBN 9781109461336

Lu, N. and Likos, W.J. (2004), *Unsaturated Soil Mechanics*, Wiley: Hoboken, NJ.

Lu, N. and Likos, W.J. (2006), "Suction stress characteristic curve for unsaturated soil", *Journal of Geotech. Geoenviron. Eng.*, Vol.132 No. 2, pp.131–142.

Muchemi, J., Mwangi, W. and Greijn, H. (2002), "GIS in support of participatory land use planning in the Districts Keiyo and Marakwet, Kenya", in *Proceedings GISDECO Seventh International Seminar on GIS in developing countries*, International Institute for Geo-Information Science and earth Observation, the Netherlands.

Norris, J.E., Stokes, A., van Beek, L.P.H., Bogaard, T., Cammeraat, E., Mickovski, S.B., Jenner, A., Di Iorio, A. and Fourcaud, T. (eds.) (2008), "Slope stability and erosion control", *Ecotechnological solutions*, pp. 65 –118.

Pack, R.T., Tarboton, D.G. and Goodwin, C.N. (2001), "Assessing Terrain Stability in a GIS using SINMAP", *The 15th Annual GIS Conference*, Vancouver, British Columbia.

Šimůnek, J., Šejna, M., Saito, H., Sakai, M. and van Genuchten M.T. (2009), "The HYDRUS-1D Software Package for Simulating the Movement of Water, Heat, and Multiple Solutes in Variably Saturated Media, Version 4.08, HYDRUS Software Series 3." Department of Environmental Sciences, University of California Riverside, Riverside, California, USA.

Standard media (2010), "Ten killed in mudslide, 20 missing after heavy rains", Updated Saturday, May 1st 2010; available *http://www.standardmedia.co.ke/business/article/2000008797/ten-killed-in-mudslide-20-missing-after-heavy-rains*; Accessed on 17th December, 2013.

Standard media (2011), "Landslide claims 3 lives as floods destroy property", Updated Saturday, December 3rd 2011 at 00:00 GMT; available: *http://www.standardmedia.co.ke/business/article/2000047721/landslide-claims-3-lives-as-floods-destroy-property*; Accessed on 17th December, 2013.

Standard media (2012), "10 killed in Marakwet landslides", Updated Saturday, December 29th 2012 at 08:49 GMT; available *http://www.standardmedia.co.ke/?articleID=2000073887*, Accessed on 17th December, 2013.

van Asch, Th. and Sukmantalya, I.N. (1993), "The modeling of soil slip erosion in the upper Komering area, South Sumatra Province, Indonesia", *Geogr. Fis. Din. Quat.* Vol.16, pp. 81-86.

van Genuchten, M.Y. (1980), "A closed form equation for predicting the hydraulic conductivity of unsaturated soils", *Soil Science Society of America Journal*, Vol. 44, pp. 892–898.

Van Westen, C.J. and Terlien, M.T.J. (1996), "Deterministic landslide hazard analysis in GIS. A case study from Manizales (Colombia)", *Earth surface processes and landforms* Vol. 21, pp. 853-868.

Vogel, C.R. and Oman, M.E. (1996), "Iterative methods for total variation denoising, SIAM", *Journal on Scientific Computing*, Vol. 17, pp. 227-238.

Vogel, T., Huang, K., Zhang, R. and van Genuchten, M.Th. (1996), "The HYDRUS code for simulating one-dimensional water flow, solute transport, and heat movement in variably-saturated media," Version 5.0, Research Report No 140, U.S. Salinity Laboratory, USDA, ARS, Riverside, CA.

YehHsin-Fu, Chen-Chang, L. and Cheng-Haw, L. (2008), "A rainfall-infiltration model for unsaturated soil slope stability", *Journal of Environmental Engineering Management*, Vol. 18 No. 4, pp. 261-268.

Yeh, H.F., Chen, J.F. and Lee, C.H. (2004), "Application of a water budget model to evaluate rainfall recharge and slope stability", *Journal of the Chinese Institute of Environmental Engineering*, Vol. 14 No. 4, pp. 227-237.

APPENDIX A. Flow chart for the infinite slope stability model

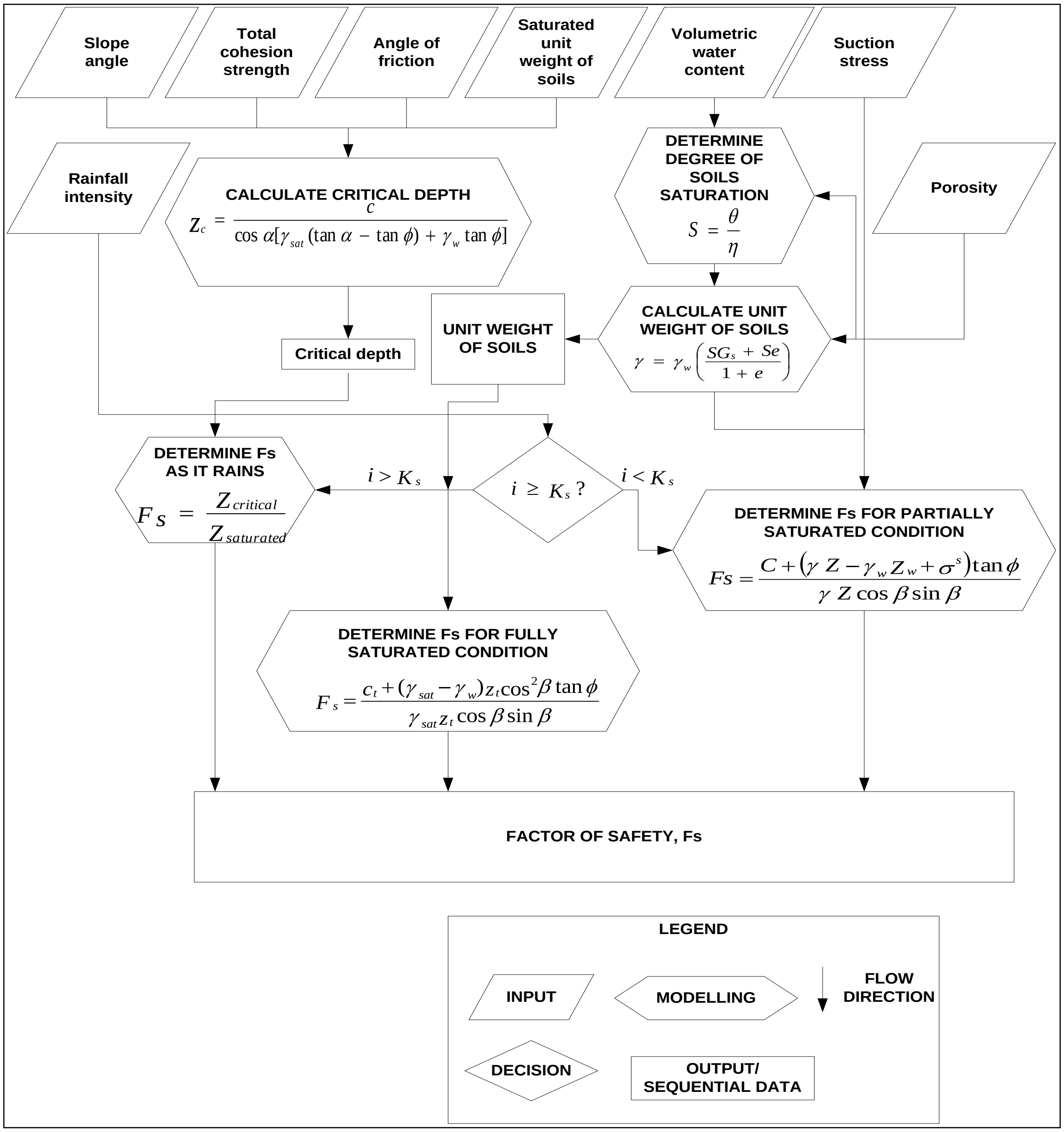

APPENDIX B. Summary flow chart of Landslide Prediction Model (LPM)